

## Inhibitor Scaffolds for 2-Oxoglutarate-Dependent Histone Lysine Demethylases<sup>†</sup>

Nathan R. Rose,<sup>†</sup> Stanley S. Ng,<sup>‡</sup> Jasmin Mecinović,<sup>†,§</sup>  
Benoît M.R. Liénard,<sup>†,§</sup> Simon H. Bello,<sup>†</sup> Zhe Sun,<sup>‡</sup>  
Michael A. McDonough,<sup>†</sup> Udo Oppermann,<sup>\*,‡</sup> and  
Christopher J. Schofield<sup>\*,†</sup>

The Department of Chemistry and the Oxford Centre for Integrative  
Systems Biology, Chemistry Research Laboratory, University of  
Oxford, 12 Mansfield Road, Oxford, OX1 3TA, United Kingdom,  
Structural Genomics Consortium, University of Oxford, Old Road  
Campus Roosevelt Drive, Headington, OX3 7DQ, United Kingdom,  
The Botnar Research Centre, Oxford Biomedical Research Unit,  
Oxford, OX3 7LD, United Kingdom

Received July 25, 2008

**Abstract:** The dynamic methylation of histone lysyl residues plays an important role in biology by regulating transcription, maintaining genomic integrity, and by contributing to epigenetic effects. Here we describe a variety of inhibitor scaffolds that inhibit the human 2-oxoglutarate-dependent JMJD2 subfamily of histone demethylases. Combined with structural data, these chemical starting points will be useful to generate small-molecule probes to analyze the physiological roles of these enzymes in epigenetic signaling.

A ubiquitous subfamily of Fe(II) and 2-oxoglutarate (2-OG)<sup>a</sup> dependent oxygenases (JmjC-domain-containing enzymes) present in all eukaryotes catalyzes the demethylation of all three N<sup>ε</sup>-methylated forms of histone lysyl residues (tri-, di-, and monomethyl) (for review, see ref 1). Demethylation is proposed to occur via methyl group hydroxylation followed by fragmentation to produce formaldehyde. Members of the JMJD2 histone demethylase subfamily are reported to display selectivity for the demethylation of transcriptionally inactivating tri- and dimethyl H3K9 (histone H3, Lys-9) and transcriptionally activating methyl-H3K36 (histone H3, Lys-36). Other JmjC subfamilies, such as the JARID subfamily, are selective for demethylation of transcriptionally activating methyl-H3K4 (histone H3, Lys-4).<sup>1</sup>

<sup>†</sup> PDB ID for crystal structure of JMJD2A complexed with inhibitor pyridine-2,4-dicarboxylic acid: 2VD7.

\* To whom correspondence should be addressed. For C.J.S.: phone, +441865275625; Fax, +441865275674; E-mail, christopher.schofield@chem.ox.ac.uk. For U.O.: phone, +441865617585; fax, +441865617575; E-mail, udo.oppermann@sgc.ox.ac.uk.

<sup>†</sup> Department of Chemistry, University of Oxford.

<sup>‡</sup> Structural Genomics Consortium and Botnar Research Centre.

<sup>§</sup> These authors contributed equally to the work.

<sup>a</sup> Abbreviations: 2-OG, 2-oxoglutarate; C-P3H, collagen prolyl-3-hydroxylase; C-P4H, collagen prolyl-4-hydroxylase; DMSO, dimethyl sulfoxide; ESI-MS, electrospray ionization mass spectrometry; FDH, formaldehyde dehydrogenase; FH, fumarate hydratase; FIH, factor inhibiting HIF; H3K4, histone H3 lysine 4; H3K9, histone H3 lysine 9; H3K36, histone H3 lysine 36; HDAC, histone deacetylase; HEPEs, (4-(2-hydroxyethyl)-1-piperazineethanesulfonic acid); HIF, hypoxia-inducible factor; JARID, Jumonji, AT-rich interactive domain; JmjC, Jumonji-C; JMJD2, JmjC-domain containing histone demethylase 2; LSD1, lysine-specific demethylase 1; MALDI-TOF MS, matrix-assisted laser desorption/ionization time-of-flight mass spectrometry; NAD<sup>+</sup>, nicotinamide adenine dinucleotide; NADH, reduced nicotinamide adenine dinucleotide; PHD, prolyl hydroxylase domain; SAHA, suberoylanilide hydroxamic acid; SDH, succinate dehydrogenase; SDS-PAGE, sodium dodecyl sulfate-polyacrylamide gel electrophoresis; SEM, standard error of the mean; TCA, tricarboxylic acid; TSA, trichostatin A.

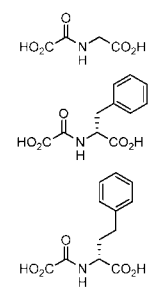
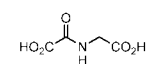
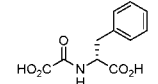
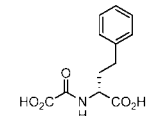
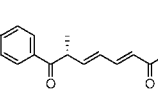
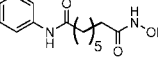
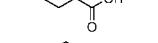
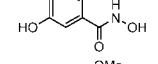
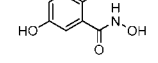
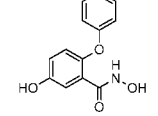
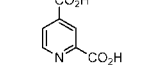
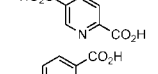
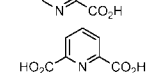
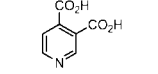
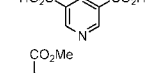
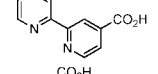
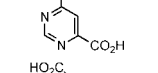
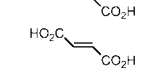
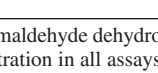
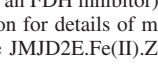
Modulation of histone modifications has significant medicinal potential. At present, the histone deacetylase (HDAC) inhibitor suberoylanilide hydroxamic acid (SAHA) is used clinically in cancer treatment<sup>2</sup> and monoamine oxidase inhibitors used in psychotherapy inhibit lysine-specific demethylase 1, LSD1, a flavin adenine dinucleotide-dependent demethylase that catalyzes demethylation of di- and monomethyl lysine residues.<sup>3</sup> Small molecules also have potential as tools to dissect the roles of epigenetic modifications of both proteins and nucleic acids, not only in cell-based studies but particularly in studying intergenerational effects. Here we report assays for inhibitors of the JMJD2 histone demethylase subfamily, with the objective of identifying different scaffolds for histone demethylase inhibition.

To identify a suitable JMJD2 enzyme for inhibition assays, we produced the recombinant forms of the catalytic domains (Supporting Information, Figure S1) of five of the six predicted human JMJD2 demethylase genes (JMJD2A, B, C, D, and E)<sup>4</sup> in *Escherichia coli* and purified them to >95% purity (by SDS-PAGE analyses, Supporting Information, Figure S2). Of the five enzymes, JMJD2E was chosen as the most suitable for inhibition work because of its stability, activity levels, and substrate selectivity profile. Kinetic assays employing MALDI-TOF (matrix-assisted laser desorption ionization-time-of-flight) mass spectrometry (MS) led to the selection of an 8-residue (ARKme<sub>3</sub>STGGK) histone H3 fragment substrate (H3K9me<sub>3</sub>). A coupled-assay for JMJD2E activity employing formaldehyde dehydrogenase (FDH) from *Pseudomonas putida* was developed based on that reported for JMJD2A.<sup>5</sup> Formaldehyde release by demethylation of the histone peptide substrate was monitored by its oxidation to give formate as catalyzed by FDH, which is carried out concomitantly with the reduction of nicotinamide adenine dinucleotide (NAD<sup>+</sup>). The production of NADH was monitored by fluorescence spectroscopy (Table 1).

Studies on the selective inhibition of 2-OG oxygenases, including the hypoxia inducible factor (HIF) hydroxylases (PHD1–3 and FIH), have identified analogues of 2-OG useful as inhibitors, including *N*-oxalyl glycine **1a** (Table 1). **1a** inhibits the human HIF prolyl hydroxylase PHD2 with  $K_i = 8 \mu\text{M}$ , and the asparaginyl hydroxylase factor-inhibiting-HIF (FIH) with  $K_i = 1.2 \text{ mM}$ .<sup>6–8</sup> **1a** inhibited JMJD2E with an IC<sub>50</sub> value of 78  $\mu\text{M}$ ; this value decreased to 24  $\mu\text{M}$  with 30 min preincubation (Table 1). Comparison of the JMJD2A·Ni(II)·Zn(II)·**1a** crystal structure<sup>9</sup> complexes with that of FIH·Fe(II)·**1b**<sup>8</sup> revealed a largely hydrophobic binding pocket adjacent to the 2-OG binding site in the JMJD2 enzymes, suggesting that stereospecific modification of **1a** at the C- $\alpha$  position may enhance inhibition or enable selectivity. *N*-Oxalyl-D-phenylalanine **1b** and *N*-oxalyl-D-homophenylalanine **1c** inhibited JMJD2E with IC<sub>50</sub> = 320  $\mu\text{M}$  and 100  $\mu\text{M}$  (39  $\mu\text{M}$  with preincubation), respectively. While these inhibitors are not more potent than **1a**, modification of **1a** to enable binding in the hydrophobic pocket enables selective inhibition of 2-OG oxygenases, as preceded for the HIF hydroxylases;<sup>12</sup> **1b** inhibits FIH with  $K_i = 83 \mu\text{M}$  but is a much less potent inhibitor of PHD2, with IC<sub>50</sub> > 1 mM.<sup>8</sup>

Both the histone deacetylases (HDACs) and the JmjC demethylases employ active site metal cofactors, Zn(II) or Fe(II), respectively, involved in catalysis. In addition to the active site Fe(II), the JMJD2 demethylases also contain a Zn binding site located close to the active site entrance.<sup>9</sup> Therefore, we then tested the known HDAC inhibitors trichostatin A (TSA, **2**),<sup>2</sup>

**Table 1.** Inhibition Data for 2-OG-Dependent Histone Demethylase JMJD2E<sup>a</sup>

Compound		IC <sub>50</sub> (μM)				Ranking of enzyme-inhibitor interaction (by ESI-MS)
		Excess 2-OG [Peptide] = K <sub>m</sub> [Fe] = 10 μM	Excess Peptide [2-OG] = K <sub>m</sub> [Fe] = 10 μM	[2-OG] = K <sub>m</sub> 30 min pre-inc	[2-OG] = K <sub>m</sub> [Fe] = 50 μM	
<b>1a</b>		830	78	24		7
<b>1b</b>		590	320	N.A.		
<b>1c</b>		270	100	39		6
<b>2</b>				28		
<b>3</b>		700	540	14	420	4
<b>4</b>		>10000	>10000			
<b>5a</b>		300	28	4.8	19	2
<b>5b</b>		300	230		160	
<b>5c</b>		340	360			
<b>6a</b>		4.7	1.4	N.A.	1.8	1
<b>6b</b>		1900	180	N.A.		
<b>6c</b>		>10000	>5000			
<b>6d</b>		250	120	N.A.	120	
<b>6e</b>		>10000	>10000			
<b>6f</b>		>10000	>10000			
<b>7</b>		24	6.6	18	8.0	3
<b>8</b>		73	27	N.A.		5
<b>9</b>		>10000	710	320		
<b>10</b>		>10000	1600	2300		

<sup>a</sup> "N.A." means that formaldehyde dehydrogenase assays were not possible due to partial inhibition of FDH by the inhibitor under pre-incubation conditions. Note that JMJD2E concentration in all assays was relatively high (2 μM) in order for sufficient NADH to be produced to be detected reliably. The IC<sub>50</sub> value reported for **2** (found to be an FDH inhibitor) was obtained by MALDI-TOF-MS, monitoring turnover of trimethyl peptide, not using the FDH coupled assay (see Supporting Information for details of methods). Assays were all carried out in triplicate, and SEMs in log(IC<sub>50</sub>) values were below 10%. The ranking of inhibitor binding to the JMJD2E·Fe(II)·Zn(II) complex was assessed by nondenaturing ESI-MS (see Supporting Information, Methods and Table S1).

suberoylanilide hydroxamic acid (SAHA, **3**), and butyric acid **4**. **4** did not inhibit JMJD2E, while **2** inhibited FDH, thus making this assay method unsuitable for **2**; assays monitoring demethylation by MALDI-TOF MS gave an IC<sub>50</sub> = 28.4 μM for **2**. **3** inhibited JMJD2E with IC<sub>50</sub> = 14 μM with preincubation.

Assays in which the Fe(II) concentration was varied indicated that the mode of inhibition by **3** was not predominantly due to Fe(II) chelation by the compound in solution. Further support for binding of **3** to JMJD2E came from nondenaturing MS analyses demonstrating that **3** bound to the JMJD2E·Fe(II)·Zn(II)

complex in a competitive manner with respect to 2-OG analogues (Supporting Information, Table S1). In contrast to a more potent inhibitor (see below), which displayed clear competitive inhibition in solution with respect to 2-OG, **3** displayed mixed inhibition in solution with respect to both 2-OG and peptide substrate. Thus we cannot be certain of how **3** binds to JMJD2E, especially given that JMJD2s contain a Zn(II) as well as an Fe(II) binding site. However, given that **3** competes with 2-OG analogues for binding to JMJD2E (Supporting Information, Table S1) and that in the enzyme–substrate complexes of both the HDACs and the JMJD2s, the terminus of the modified lysine side chain binds close to Zn(II) and Fe(II), respectively, it seems possible that the hydroxamic acid of **3** binds to the Fe(II) of JMJD2E. **3** is reported to inhibit HDAC1 with an  $IC_{50} = 48$  nM;<sup>10</sup> thus based on inhibition data in vitro, **3** is likely to be selective for HDACs over the JMJD2s; however, there is at least a possibility of a dual-enzyme family inhibition mechanism operating in vivo for **3** and, possibly, for other HDAC inhibitors that are metal chelators.

Following analysis of JMJD2A-substrate-complex crystal structures<sup>9</sup> (JMJD2A and JMJD2E have ~65% identity over their catalytic domains), we proposed and synthesized low molecular weight aromatic hydroxamic acids (**5a–5c**) intended to chelate the Fe(II) of JMJD2E in a manner similar to that predicted for **3**. **5a** was the most potent of these compounds, with  $IC_{50} = 4.8$   $\mu$ M, and was significantly more active than **3**. Variation in the Fe(II) concentration indicated that **5a** is a 2-OG competitor and that inhibition was not predominantly due to Fe(II) chelation in solution. We also investigated several pyridine carboxylates (**6a–6f**), some of which are known inhibitors of collagen and HIF prolyl hydroxylases.<sup>11</sup> Pyridine-2,4-dicarboxylic acid **6a** was the most potent JMJD2E inhibitor tested, with  $IC_{50} = 1.4$   $\mu$ M, and  $K_i = 914 \pm 85$  nM (competitive inhibition with respect to 2-OG). Inhibition of other Fe(II)/2-OG dependent oxygenases using **6a** has been reported for the collagen prolyl-4-hydroxylase (C–P4H) ( $K_i = 2$   $\mu$ M), the collagen prolyl-3-hydroxylase (C–P3H) ( $K_i = 9$   $\mu$ M)<sup>12</sup> and for the HIF prolyl hydroxylases PHD1–3 ( $K_i = 7–40$   $\mu$ M).<sup>6</sup> In contrast, pyridine-2,5-dicarboxylic acid **6b** is more potent as an inhibitor of C–P4H ( $K_i = 0.8$   $\mu$ M) but displays no significant inhibition of C–P3H ( $K_i > 1000$   $\mu$ M), the PHD enzymes ( $K_i > 300$   $\mu$ M) nor of JMJD2E ( $IC_{50} = 184$   $\mu$ M). The bicyclic analogue **7** [4'-(methoxycarbonyl)-2,2'-bipyridine-4-carboxylic acid] and the pyrimidine analogue **8** also inhibited JMJD2E effectively, with  $IC_{50} = 6.6$   $\mu$ M and  $IC_{50} = 27$   $\mu$ M respectively.

Variants of the TCA cycle enzymes, succinate dehydrogenase (SDH) and fumarate hydratase (FH), lead to elevated intracellular levels of succinate **9** and fumarate **10**, which are proposed to stimulate tumor growth by activation of the hypoxic response via HIF hydroxylase inhibition.<sup>13,14</sup> Cellular levels of **9** and **10** in SDH- and FH-deficient tumor cells are estimated at 30–100  $\mu$ mol/g protein and 400–600  $\mu$ mol/g protein respectively.<sup>13</sup> **9** and **10** were relatively poor inhibitors of JMJD2E, with  $IC_{50} = 0.32$  mM (**9**, preincubation) and 2.3 mM (**10**). Smith et al. have reported apparent inhibition of JMJD2D activity by high concentrations of **9** (1–10 mM) in cells.<sup>15</sup> However, the weak inhibition of JMJD2E by **9** and **10** contrasts with the more potent inhibition of a HIF prolyl hydroxylase (PHD2) by **10** ( $IC_{50} = 3$   $\mu$ M, preincubation) and by **9** ( $IC_{50} = 19$   $\mu$ M, preincubation).<sup>16</sup> However, FIH, which is much more closely related to the histone demethylases in sequence and structure than are the PHDs, was only weakly inhibited by **9** and **10** ( $IC_{50} > 1$  mM). Thus, the available data, albeit limited, suggest that cellular effects involving 2-OG oxygenase inhibition by **9** and **10** are more

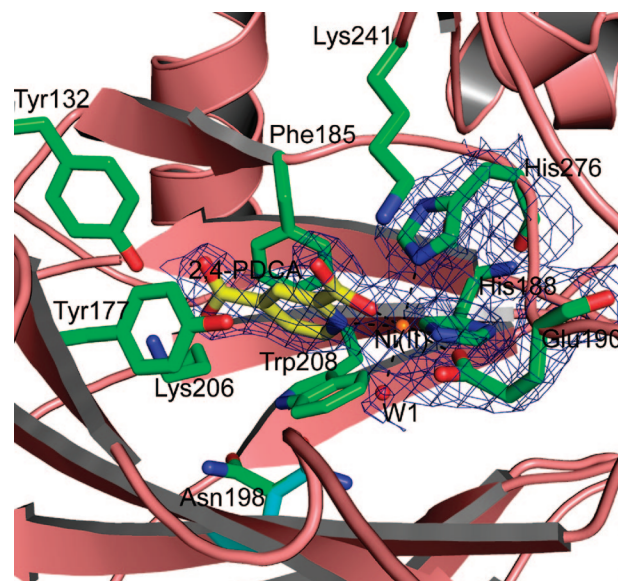


**Figure 1.** View from a crystal structure of JMJD2A·Ni(II)·Zn(II) (pink and green) complexed with **6a** (yellow) [PDB ID 2VD7]. The experimental  $2F_o - F_c$  electron density, displayed as blue mesh, is shown for the metal coordinating residues and ligands (contoured to  $1.5\sigma$ ). **6a** interacts with the Ni(II) ion (orange, substituting for Fe(II)) via bidentate coordination; the pyridinyl nitrogen coordinates to the metal *trans* to O<sup>e1</sup> of Glu-190 (2.3 Å), and one of the **6a** 2-carboxylate oxygens, O2, coordinates the metal *trans* to His-276 (2.2 Å). The pyridine ring of **6a** is positioned to form hydrophobic interactions with Tyr-177, Phe-185, and Trp-208. The non-metal-ligated 2-carboxylate oxygen of **6a** is positioned to hydrogen bond with N<sup>e</sup> of Lys-241 (3.1 Å) and the Tyr-177 OH (3.5 Å) and likely interferes with methyl–lysine substrate binding (see Supporting Information, Figure S7). The six-coordinate metal coordination is completed by a water molecule (W1, O to Fe: 2.3 Å). The 4-carboxylate oxygens of **6a** interact with the 2-OG 5-carboxylate binding residues, Lys-206 N<sup>e</sup> (2.8 Å) and Tyr-132 OH (2.6 Å). Asn-198 was observed in two alternative conformations (green and cyan sticks), one of which is positioned to form a hydrogen bond with the metal coordinated water.

likely to be mediated via inhibition of the HIF prolyl hydroxylases rather than FIH or the analyzed histone demethylases.

Electrospray ionization (ESI)-MS analyses under non-denaturing conditions (Supporting Information, Figure S3) verified binding of the inhibitors to the JMJD2E·Fe(II)·Zn(II) complex. Competitive binding experiments were then used to rank the most potent inhibitors qualitatively in terms of binding affinity for JMJD2E (Table 1, Supporting Information, Table S1). In these competitive experiments, the seven inhibitors observed to bind the best in the initial MS analyses were ranked by experiments in which pairs of inhibitors were mixed with JMJD2E and allowed to compete with each other for protein binding. The results of this ranking of binding affinity correlated reasonably well with the  $IC_{50}$  values obtained in solution, with **6a** having the highest affinity for the enzyme (rank order of binding strength by MS: **6a** > **5a** > **7** > **3** > **8** > **1c** > **1a**, compared to **6a** > **5a** > **3** > **7** > **8** > **1a** > **1c** by FDH inhibition assay  $IC_{50}$ s).

To examine the mode of binding of the most potent inhibitor identified, a crystal structure of the JMJD2A·Ni(II)·Zn(II)·**6a** complex was determined to 2.0 Å resolution (a crystal structure of JMJD2E has not yet been obtained). The structure (Figure 1) reveals that pyridine-2,4-dicarboxylic acid **6a** binds to JMJD2A between the  $\beta$ -sheets of its double stranded  $\beta$ -helix fold in a different metal coordination mode to that observed for *N*-oxalylglycine **1a**.<sup>9</sup> It binds to the Ni(II) [which replaces Fe(II)] in a bidentate manner via its N-atom and 2-carboxylate



and occupies the 2-OG binding site in the enzyme. This binding mode is consistent with our kinetic analyses, showing that **6a** is a competitive inhibitor with respect to 2-OG. There was no evidence for any binding of **6a** at the Zn(II) site, which is present in both JMJD2A and JMJD2E. **6a** was also shown to inhibit JMJD2A in an FDH coupled assay with  $IC_{50} = 0.7 \mu M$  (although the data quality for JMJD2A was inferior to that for JMJD2E, possibly due to lower levels of enzyme activity).

Overall we have identified inhibitors of the JMJD2 histone demethylases, of which the most potent is **6a**. Other identified inhibitors that are also 2-OG analogues include the hydroxamic acid **5a** and the oxalylamino acids **1a** and **1c**, all of which should provide starting points for the development of more potent inhibitors. Notably, the known HDAC inhibitors **3** and **2** also inhibit the JMJD2 histone demethylases, albeit much less potently than they inhibit the HDAC enzymes. Succinate **9** and fumarate **10**, TCA cycle intermediates potentially implicated in tumor growth,<sup>13,15,16</sup> do not display significant inhibition of the analyzed JMJD2 demethylases. Although the more potent inhibition of other demethylases cannot be ruled out, the available evidence suggests that the role in this effect is more likely to involve the inhibition of the HIF prolyl hydroxylases than the histone demethylases. Our work marks a starting point for the development of small-molecule inhibitors of the histone demethylases for use as therapeutic agents and as chemical tools for investigating the complex interplay between the many enzymes involved in epigenetics.

**Acknowledgment.** Help with synchrotron data collection by F. von Delft is gratefully acknowledged. We thank the Commonwealth Scholarship Commission, The Wellcome Trust, and the BBSRC for funding. The Structural Genomics Consortium is a registered charity (no. 1097737) that receives funds from a number of sources, details of which are found in the Supporting Information.

**Supporting Information Available:** Sequence alignments of JMJD2 histone demethylases, reactions catalyzed by histone demethylases, cloning and expression of JMJD2E, peptide synthesis, inhibitor synthesis, inhibition assay methods, mass spectrometric data, and crystallization and structure solution methods. This material is available free of charge via the Internet at <http://pubs.acs.org>.

## References

- (1) Klose, R. J.; Zhang, Y. Regulation of histone methylation by demethylination and demethylation. *Nat. Rev. Mol. Cell Biol.* **2007**, *8*, 307–318.
- (2) Marks, P. A.; Breslow, R. Dimethyl sulfoxide to vorinostat: development of this histone deacetylase inhibitor as an anticancer drug. *Nat. Biotechnol.* **2007**, *25*, 84–90.
- (3) Lee, M. G.; Wynder, C.; Schmidt, D. M.; McCafferty, D. G.; Shiekhata, R. Histone H3 Lysine 4 Demethylation Is a Target of Nonselective Antidepressive Medications. *Chem. Biol.* **2006**, *13*, 563–567.
- (4) Katoh, M.; Katoh, M. Identification and characterization of JMJD2 family genes in silico. *Int. J. Oncol.* **2004**, *24*, 1623–1628.
- (5) Couture, J.-F.; Collazo, E.; Ortiz-Tello, P. A.; Brunzelle, J. S.; Trievel, R. C. Specificity and mechanism of JMJD2A, a trimethyllysine-specific histone demethylase. *Nat. Struct. Mol. Biol.* **2007**, *14*, 689–695.
- (6) Hirsila, M.; Koivunen, P.; Gunzler, V.; Kivirikko, K. I.; Myllyharju, J. Characterization of the human prolyl 4-hydroxylases that modify the hypoxia-inducible factor. *J. Biol. Chem.* **2003**, *278*, 30772–30780.
- (7) Ivan, M.; Haberberger, T.; Gervasi, D. C.; Michelson, K. S.; Gunzler, V.; Kondo, K.; Yang, H.; Sorokina, I.; Conaway, R. C.; Conaway, J. W.; Kaelin, W. G., Jr. Biochemical purification and pharmacological inhibition of a mammalian prolyl hydroxylase acting on hypoxia-inducible factor. *Proc. Natl. Acad. Sci. U.S.A.* **2002**, *99*, 13459–13464.
- (8) McDonough, M. A.; McNeill, L. A.; Tilliet, M.; Papamicael, C. A.; Chen, Q. Y.; Banerji, B.; Hewitson, K. S.; Schofield, C. J. Selective inhibition of factor inhibiting hypoxia-inducible factor. *J. Am. Chem. Soc.* **2005**, *127*, 7680–7681.
- (9) Ng, S. S.; Kavanagh, K. L.; McDonough, M. A.; Butler, D.; Pilka, E. S.; Lienard, B. M. R.; Bray, J. E.; Savitsky, P.; Gileadi, O.; von Delft, F.; Rose, N. R.; Offer, J.; Scheinost, J. C.; Borowski, T.; Sundstrom, M.; Schofield, C. J.; Oppermann, U. Crystal structures of histone demethylase JMJD2A reveal basis for substrate specificity. *Nature* **2007**, *448*, 87–91.
- (10) Belvedere, S.; Witter, D. J.; Yan, J.; Secrist, J. P.; Richon, V.; Miller, T. A. Aminosuberoyl hydroxamic acids (ASHAs): a potent new class of HDAC inhibitors. *Bioorg. Med. Chem. Lett.* **2007**, *17*, 3969–3971.
- (11) Tschank, G.; Brocks, D. G.; Engelbart, K.; Mohr, J.; Baader, E.; Gunzler, V.; Hanauske-Abel, H. M. Inhibition of prolyl hydroxylation and procollagen processing in chick-embryo calvaria by a derivative of pyridine-2,4-dicarboxylate. *Biochem. J.* **1991**, *275*, 469–476.
- (12) Tiainen, P.; Pasanen, A.; Sormunen, R.; Myllyharju, J. Characterization of recombinant human prolyl 3-hydroxylase isoenzyme 2, an enzyme modifying the basement membrane collagen IV. *J. Biol. Chem.* **2008**, *283*, 19432–19439.
- (13) Pollard, P. J.; Briere, J. J.; Alam, N. A.; Barwell, J.; Barclay, E.; Wortham, N. C.; Hunt, T.; Mitchell, M.; Olpin, S.; Moat, S. J.; Hargreaves, I. P.; Heales, S. J.; Chung, Y. L.; Griffiths, J. R.; Dalgleish, A.; McGrath, J. A.; Gleeson, M. J.; Hodgson, S. V.; Poulosom, R.; Rustin, P.; Tomlinson, I. P. M. Accumulation of Krebs cycle intermediates and over-expression of HIF1{alpha} in tumours which result from germline FH and SDH mutations. *Hum. Mol. Genet.* **2005**, *14*, 2231–2239.
- (14) Selak, M. A.; Armour, S. M.; MacKenzie, E. D.; Boulahbel, H.; Watson, D. G.; Mansfield, K. D.; Pan, Y.; Simon, M. C.; Thompson, C. B.; Gottlieb, E. Succinate links TCA cycle dysfunction to oncogenesis by inhibiting HIF- $\alpha$  prolyl hydroxylase. *Cancer Cell* **2005**, *7*, 77–85.
- (15) Smith, E. H.; Janknecht, R.; Maher, L. J., III. Succinate inhibition of {alpha}-ketoglutarate-dependent enzymes in a yeast model of paraganglioma. *Hum. Mol. Genet.* **2007**, *16*, 3136–3148.
- (16) Hewitson, K. S.; Lienard, B. M.; McDonough, M. A.; Clifton, I. J.; Butler, D.; Soares, A. S.; Oldham, N. J.; McNeill, L. A.; Schofield, C. J. Structural and mechanistic studies on the inhibition of the hypoxia-inducible transcription factor hydroxylases by tricarboxylic acid cycle intermediates. *J. Biol. Chem.* **2007**, *282*, 3293–3301.

JM800936S